Journal of Applied Fluid Mechanics, Vol. 16, No. 10, pp. 2019-2029, 2023.
Available online at www.jafmonline.net, ISSN 1735-3572, EISSN 1735-3645.
https://doi.org/10.47176/jafm.16.10.1796

Simulation of the Hydraulic Performance of Parallel Pivot Weirs with Different Angles

B. Khatamipour[1], A. Khosrojerdi[1†], M. R. Kavianpour[2] and M. Ghodsi Hassanabad[1]

[1] *Science and research Branch, Islamic Azad University, Tehran, Iran*
[2] *KN Toosi University of Technology, 470 Mirdamad Ave. west, Tehran, Iran*

†Corresponding Author Email: khosrojerdi@srbiau.ac.ir

ABSTRACT

Pivot weirs are one of the most important structures for regulating the water level in rivers and canals. These weirs are constructed with one or more gates in a row in the waterways. Changing the angle of each gate is done individually with an independent system. Based on available information, the hydraulic performance of this type of weirs (especially in several gates and different angles) in different operational conditions has not been investigated. In present study, pivot weirs with two gates are simulated using Ansys CFX software with the angles of 27.8 to 90 degree and the discharges between 40 to 130 L/s. Further, the importance of the open space between the two adjacent weirs with different angles (lack of retail wall) and its hydraulic behavior have been studied. The model was calibrated based on valid laboratory data and using the K-ϵ turbulence model. Therefore, the weirs with equal angles were studied in the first step. In this case, the effective discharge angle coefficient was studied and its maximum value compared to the vertical angle was obtained 1.076 for the angle of 52°. Furthermore, relationships for discharge coefficient versus upstream water depth were developed. In the next step, the effective length of the crest was found to be increases by 30% under unequal angles operation and the discharge coefficient raised by 1.3 to 2.4 times. Also, it was recognized that, in case of two weirs with unequal angles, about 26% to 69% of the flow passes through the distance between the two weirs. Therefore, the performance of unequal angles operation seems to be more effective in controlling the water level and discharge in different conditions and especially in flood events.

Article History

Received February 2, 2023
Revised May 7, 2023
Accepted May 22, 2023
Available online July 29, 2023

Keywords:

Ansys CFX
Pivot Weir
K-ε Turbulence Model
Discharge Coefficient
Free flow

1. INTRODUCTION

Pivot weirs are a combination of plates and hydraulic jacks. This system provides the possibility of various blocking the flow for storage purposes behind and discharging the reservoirs during flood events. The weirs can be adjusted by a remote sensing system. Due to the connection of the gates to the channel floor, retaining wall between the adjacent gates is eliminated (Fig. 1).

The discharge equation for vertical sharp-crested weirs is:

$$Q = \frac{2}{3}.C_d.\sqrt{2g}.b.H \wedge (1.5) \qquad (1)$$

where, C_d is the discharge coefficient (-), b is length of weir(m), H is water head over the crest(m) and Q is the discharge(m^3/s). Kindsvater and Carter (1959) corrected Eq. (1) by removing the effect of viscous and surface forces. In addition, they stated that if an effective factor of weir angle (C_a) is correctly estimated, by multiplying it in Eq. (1), the equation of inclined weirs is obtained. For this

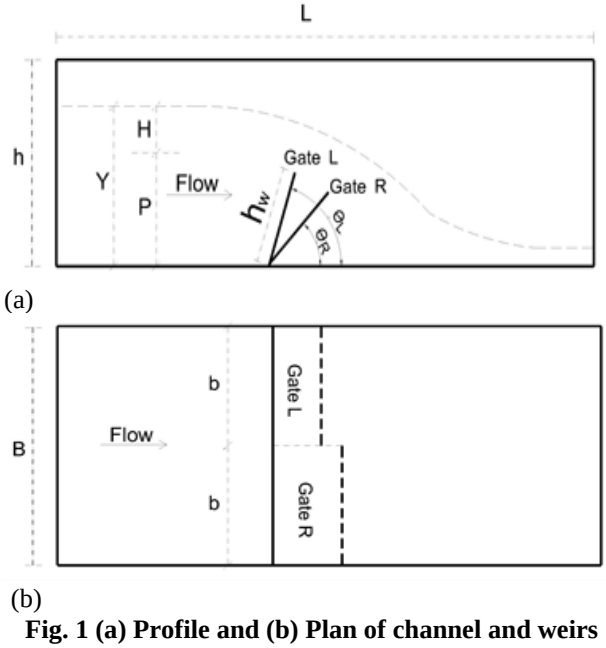

Fig. 1 (a) Profile and (b) Plan of channel and weirs

purpose, experimental studies of Wahlin and Replogle (1994) with the support of USBR Institute, on flume with a width of 1.23m and for two pivot weirs with the widths of 1.2 and 1.14m and the heights of 0.61m (Armtec gates) and 0.46m (USWCL gates) were used. Their experiments had performed on Armtec gates for angles between 16.2 and 62.4 degree and flow discharges in the range of 15.7 to 170 lit/s. Finally, they presented the following discharge equation of rectangular pivot weir for free-flow:

$$Q = 2/3.C_a.C_r.C_d.\sqrt{2g}.[(H+k_h)(b+k_b) - 2A_s.Cos\theta]\sqrt{H+k_h} \quad (2)$$

$$C_a = 1.0333 + 0.003848\theta - 0.000045\theta^2 \quad (3)$$

where, K_h and K_b are, respectively, the correction factors of H and b (m), C_a is the effective coefficient of the angle, C_r is the effective coefficient due to the roundness of the crest, A_s is the area of seals (m^2) and θ is the weir angle relative to the channel floor(degree). According to the results obtained, by reducing the angle to 40 degree, the discharge coefficient had an increasing trend, and with a further decrease in the angle, this trend was decreasing. Manz (1985) evaluated the simulation model of the irrigation conveyance system for pivot weirs and presented the following equation for the coefficient C_a:

$$C_a = -10^{-12}\times 5.89\theta^6 + 10^{-9}\times 1.202\theta^5 - 10^{-8}\times 8.35\theta^4 + 10^{-6}\times 3.422\theta^3 - 10^{-4} * 2.217\theta^2 + 10^{-3}\times 9.035\theta + 1 \quad (4)$$

Godderidge et al. (2004) performed surface free flow simulation, using Ansys CFX software on gas tanks, high speed craft, and propellers of underwater vehicles. They stated successful validation of the model for multiphase flows. Arvanaghi and Oskuei (2013) performed numerical studies of flow over sharp-crested weirs without side contraction using FLUENT software. In this study, the volume control method and *RNG K-ε* turbulence model were used. Abdolahpour et al. (2013) studied the broad-crested weirs with upstream and downstream sloping with FLUENT software. They reported that *K-ε* model shows reasonable accuracy for predicting water surface profile and hydraulic behavior. Zachoval and Roušar (2015) conducted experimental and numerical studies to simulate the flow over wide edge weirs. They compared different types of turbulence models using Ansys CFX software. According to the results, Ansys CFX shows accurate results in calculating different hydraulic parameters. Sheikh Rezazadeh Nikou et al. (2016) investigated pivot weir for free-flow conditions. The difference between their proposed equations and the laboratory results was found to be about 15%. Kulkarni and Hinge (2017, 2020) studied compound broad crested (CBC) weir. They designed CBC weir, which effectively measures various discharges and maintains a constant discharge coefficient (independent of H). The proposed formula showed good agreement with the laboratory measured discharge in the range of 2.6% mean error. They also performed CFD simulations on this weir with Flow3D software in 2020 , 2021, using renormalized group (RNG) approach. The model was validated based on laboratory results. They modified the shape of weir to achieve constant C_d and verified the numerical performance of the CBC weir for measuring different discharges (based on a constant value of 0.6 for discharge coefficient), using the experimental measurements. Ahmed and Aziz (2018) simulated side spillway weirs with Ansys CFX. They reported that the *K-ε* and *RNG k-ε* models show high accurate results for different discharges. Bijankhan and Ferro (2018) carried out experimental and numerical studies to check the effect of θ for rectangular weir in free-flow conditions. They acknowledged on the highest value of C_a=1.082 for θ=30. In their study, numerical analysis was performed with OpenFOAM software and *K-ε* turbulence model. They suggested the following equation for C_a based on a constant upstream water depth:

$$C_a = \left(1+\frac{0.041*\theta^{-21.348}}{206.9+0.759963\theta^{-21.348}}\right)^{3/2} \quad (5)$$

Shawnm and Sarhang (2019) conducted research to validate the Ansys CFX software for simulating flow over stepped spillway. They used RNG K-ε turbulence model. The results showed good agreement between the laboratory and the model outputs. Gong et al. (2019) conducted experimental study on four different shapes of sharp-crested and rounded-crested vertical weirs. They presented a direct relation for C_d in terms of crest roundness and *H/P*. The results showed that the upstream roundness edge of the weir crest increases the discharge coefficient. Mahdavi et al. (2020) performed SPH analysis on pivot weirs and showed that the position of the vena contracta is transferred downstream for steep weir slopes. They proposed the following equation:

$$C_a = 6.33*10^{-7}\theta^3 - 6.929*10^{-5}\theta^2 - 0.001768\,\theta + 0.9308 \quad (6)$$

As a conclusion, the history of the previous studies showed an emphasis on the performance of different types of single weirs using different softwares. In other words, little information is available on pivot weirs with two adjacent gates and different angles, which provides flexible operation during emergency flood situation. Therefore, the main objective of this study is to numerically study two parallel pivot weirs to check the effect of weir angles on their hydraulic performance and discharge coefficients. For this purpose and based on the main features of Ansys CFX, it was used for simulation. The model uses different turbulence methods and is capable of 2D and 3D multi-phase flow simulation, considering moving structures, and fluid structure interaction (FSI). In line with the points addressed above, the result of this research with more focus on pivot weirs including two gates can help operating and maneuvering the gates in emergency conditions and floods conditions. To achieve the objectives, the evaluation of Ansys CFX software was accomplished (Khatamipour et al. 2022a, b).

2. MATERIALS AND METHODS

The present study was performed in two steps. In the first step, calibration of the model was done based on the Wahlin and Replogle's experimental data on Armtec gates. The methodology and the results of model calibration (with more details) are fully explained in Khatamipour et al. (2022a, b). However, a summary of the results and also the results of model for pivot weirs with two gates are presented, hereafter.

Table 1 Output results of the model calibrated by experimental data of Armtec gates

Geometry and hydraulics parameters	Unit	Run No.				
		1	2	3	4	5
Q	lit/s	62.22	65.35	27.92	149.57	61.47
θ	degree	63.4	43.6	43.6	22.4	22.4
Y_{Ansys}	cm	52.5	44.3	39.7	37.8	29.6
Y_{Arm}		52.3	43.7	39.6	36.3	29.4
RE	%	0.3	1.3	0.2	4.4	0.6
RMSE	-	0.17	0.56	0.09	1.58	0.18

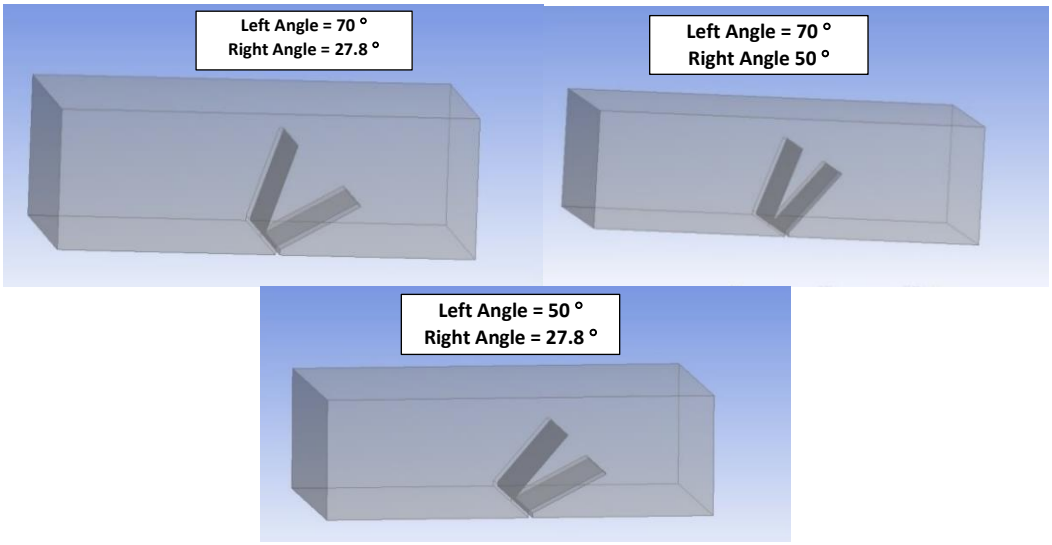

Fig. 2 Flume and pivot weir

2.1 Governing Equations and Problem-Solving Approaches

Navier-Stokes equations are the most comprehensive equations governing fluid motion. These equations are presented as follows for the analysis of the flow in the channels (which is the turbulent water-air two-phase flow) (Liu et al. 2002):

$$\frac{\partial}{\partial t}(\rho u_j) + \frac{\partial}{\partial x_i}(\rho u_i u_j) = -\frac{\partial P}{\partial x_j} + \frac{\partial}{\partial x_i}(\mu + \mu_t) * \left(\frac{\partial u_i}{\partial x_j} + \frac{\partial u_j}{\partial x_i}\right) + \rho g \quad (7)$$

$$\rho = \alpha_A \rho_A + \alpha_w \rho_w \quad (8)$$

$$\mu = \alpha_A \mu_A + \alpha_w \mu_w \quad (9)$$

in which, u_i and u_j are the flow velocity components, α_A and α_W are the ratios of air and water, respectively, ρ_A, ρ_W, and ρ are respectively the density of air, water and air-water mixture, μ_t and μ are respectively the viscosity of turbulence and the air-water mixture, μ_A and μ_W are the viscosity of air and water, respectively and k is the turbulent kinetic energy.

2.2 Non- Dimensional Parameter

Based on non-dimensional analysis, the following equation between discharge coefficient (C) and effective parameters can be distinguished:

$$C = f(H/P, b/B, \theta, F_r) \quad (10)$$

where, F_r is Froud number. By measuring the hydraulic parameters, relationship between discharge coefficient and the dimensionless parameters is extracted.

2.3 Model Calibration

The model was run for different weir angles and flow discharges based on the experimental results. The angles and flow discharges were selected based on the maximum, medium, and minimum values. According to the laboratory model, the flume width and the weir length were 123 and 114cm, respectively (lateral contraction equal to 0.925). After examining different turbulence models, standard *K-ε* method was selected. Then model accuracy was analyzed (Khatamipour et al. 2022a, b). The model output results are presented in Table 1.

In the table 1, the "*Arm*" and "*Ansys*" indices represent the laboratory data and model results, respectively. The relative error (RE) and the root mean square error (RMSE) was respectively calculated between 0.2 to 4.4% and 0.17 to 1.58, which showed reasonable performance of the model.

2.4 Pivot Weirs with Two Gates

The geometry, including flume and weirs, was drafted in Ansys workbench (Fig. 2). The geometrical specifications and hydraulic parameters are presented in Table 2. According to the previous investigations, the minimum water depth on the crest to avoid scale

Table 2 Geometric specifications of the model and hydraulic parameters

Flow discharge (lit/s)	Angle (°)	Weir dimensions (cm)			Flume dimensions (cm)		
Q	Y	t	b	h_w	h	B	L
130, 80, and 40	90, 70, 50, and 27.8	2	60	40	65	120	200

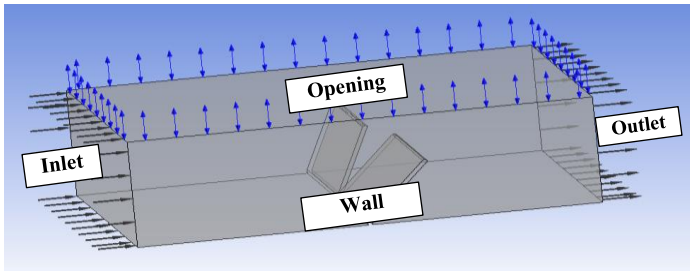

(a)

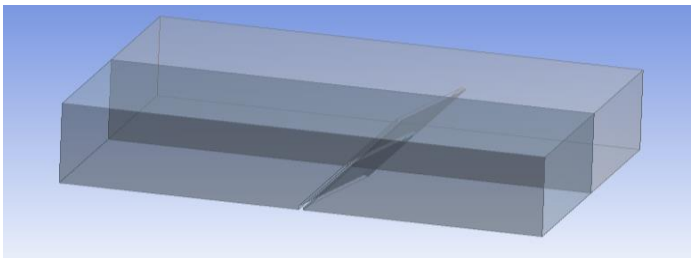

(b)

Fig. 3 (a) Position of Inlet, Outlet, Opening and Wall borders & (b) symmetry border

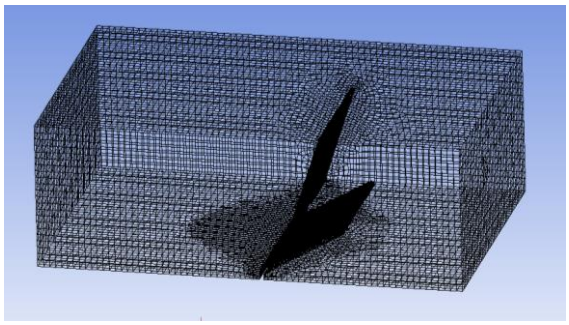

Fig. 4 Meshing

and viscosity effects is 1 to 2 cm, which was take into account in geometrical consideration. Also, the angles of adjacent weirs for θ=90° are basically equal for modeling the pivot weir.

2.4.1 Boundary Conditions

Domain boundary were divided into different areas as follows (Fig. 3(a)):

- **Inlet** is used to introduce the flow entry, where the flow discharge is determined.

- **Outlet** shows the outflow at downstream, where static pressure is set as zero.

- **Opening** is the open surface in the upper part of the domain, where zero relative pressure is set for it.

- **Wall** is the solid surfaces which limits the flow range (including channel body and weir), where no-slip condition is satisfied.

* In case, where $\theta_L=\theta_R$ (the weirs angles are equal), the symmetry condition is defined at the interface of the two weirs (Fig. 3(b)).

2.4.2 Mesh Layout

In order to increase the accuracy, the domain was divided into several sections and different mesh size was defined for each (Fig. 4). The optimal mesh dimensions were determined based on the sensitivity analysis.

3. RESULTS AND DISCUSSION

Where the left and right weir angles are equal, due to structural conditions and lack of retaining wall between the adjacent weirs (Fig. 1), the model was considered as a single weir. In the first step, this condition was considered as initial case and their hydraulic conditions were analyzed. Then, in the second step, weirs with unequal angles were analyzed and the effect of angle on discharge coefficients and its variation with respect to the initial case was assessed. Finally, the importance of retaining wall between two weirs is discussed.

3.1 Equal Angles (First Step)

In this condition, the geometry of the flow is symmetrical. Therefore, the model was run by considering a symmetry plane for half of the flume. The results of water surface profile for θ=70° is shown in Fig. 5. In order to compare and analyze the results with previous investigations and also to check the effect of angle on discharge coefficient (C), the results were determined in the form of $C_a=C/C_{90}$. The shape of the flume and the symmetry plane are shown in Fig. 3(b).

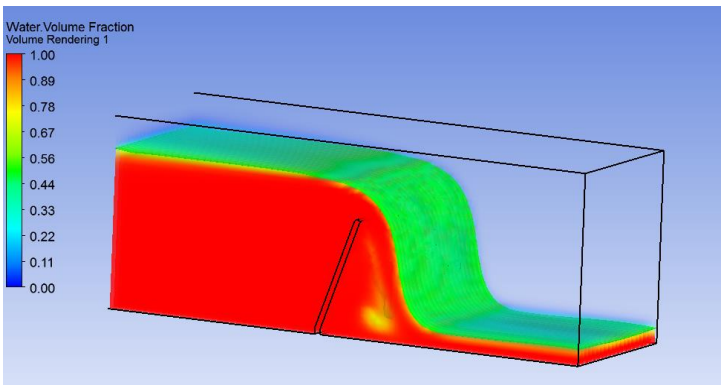

Fig. 5 Water surface profile over the weir with an angle of 70 degree

Table 3 Calculation of discharge coefficient of pivot weirs

Geometry and hydraulics parameters	Number of runs											
	1	2	3	4	5	6	7	8	9	10	11	12
Type	L90- R90			L70- R70			L50- R50			L27.8- R27.8		
Q (lit/s)	130	80	40	130	80	40	130	80	40	130	80	40
$P_{L,R}$ (cm)	41.6	41.6	41.6	39.9	39.9	39.9	33.8	33.8	33.8	22.7	22.7	22.7
$b_{L,R}$ (cm)	60	60	60	60	60	60	60	60	60	60	60	60
Y (cm)	59.4	53.7	48.1	57.0	51.5	46.3	50.8	45.6	40.2	39.9	34.7	29.2
H (cm)	17.8	12.0	6.5	17.1	11.6	6.4	17.0	11.8	6.4	17.2	12.0	6.5
C (-)	0.487	0.540	0.680	0.519	0.568	0.698	0.524	0.557	0.696	0.515	0.543	0.689
C_a (-)	1.000	1.000	1.000	1.067	1.053	1.026	1.076	1.033	1.024	1.058	1.007	1.012

The results for equal angles of θ=90°, 70°, 50°, and 27.8° are presented in Table 3.

In Table 3, the indices L and R correspond to the left and right weirs (in the flow direction). The term L70-R70 indicates the location of the weirs and their angles. Considering that the C_a for the weir with an angle of 90 degree is equal to 1, the value of the effective angle coefficient ($C_a=C/C_{90}$) was calculated and the results are presented in Table 3. The trend of changes in the coefficient C_a for different flow discharges is shown in Fig. 6.

Variation of C_a-θ in Fig. 6 shows that the weir discharge coefficient (C_a) increases with θ=52°, but then reducing with further increasing the weir angle. The maximum value of C_a was calculated as 1.076, indicating a slight difference from Wahlin (1994), Manz (1985), and Bijankhan (2018), which reported C_a equal to 1.121,

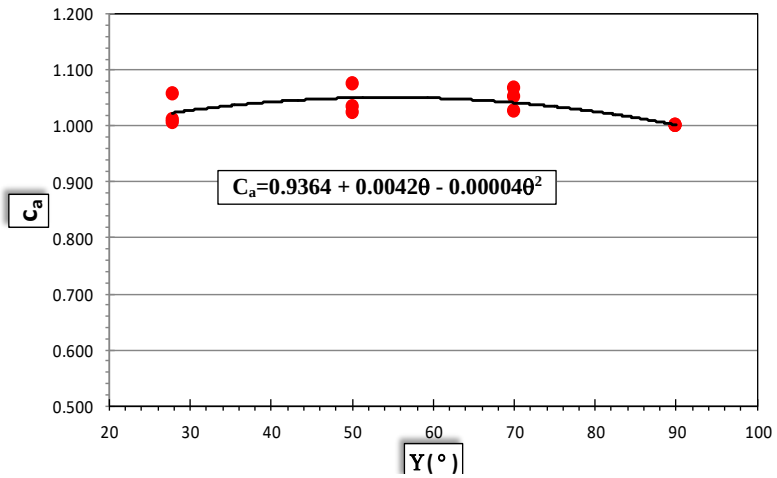

Fig. 6 Variation of coefficients C_a versus θ

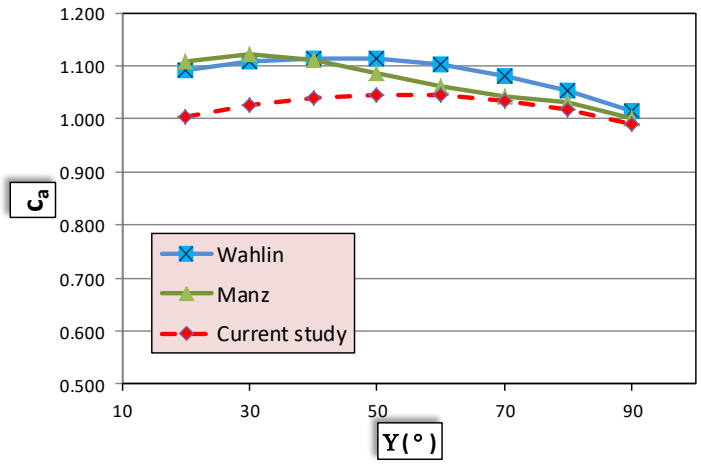

Fig. 7 Variation of coefficient C_a in different studies

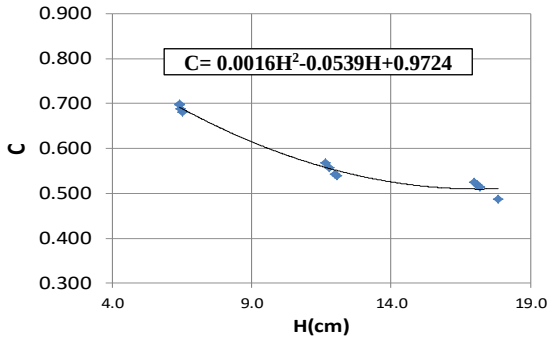

Fig. 8 Variation of C versus H and H/P

1.110, and 1.082, respectively. The present study shows the maximum weir discharge coefficient increase by 7.6%. The reason for this difference can be due to the shape of the crest and side contraction of the weirs in different studies. The comparison of C_a based on previous studies (Eqs. (3) and (4)) with the present results is also shown in Fig. 7.

According to the results in Table 3, the variation of weir discharge coefficients (C) versus H as shown in Fig. 8 exhibits a decreasing trend.

Figure 8 also shows the possibility of developing equation with correlation coefficient greater than 0.9 and independent of the weir angle. The results for the extracted equation is used in weir analysis with unequal angles in the next step.

3.2 Unequal Weir Angles (Second Step)

In the following section, the effect of only one weir angle changes is provided. The model results for the weirs with unequal angles are presented in Table 4.

A sample of water surface profile is also shown in Fig. 9. In Table 4, θ_r is the ratio of right to left weir angles (θ_R/θ_L), C_{avg} is the weighted average of the weir discharge coefficient, which is based on the new length of the crests. For weirs with equal angles (θ_r=1), C_{avg} is the discharge coefficient (C), as given in Table 3.

In Table 4, C_{avg} is the weighted average of the weir discharge coefficient in the cross-section, which is calculated based on the new length of the crests. In the series of weirs with equal angles (θ_r=1), C_{avg} is equal to the calculated discharge coefficient (C) in table 3.

According to Fig. 9, by reducing the angle of right weir, an excess flow also passes through the empty space between the two weirs. In this study, an effective length

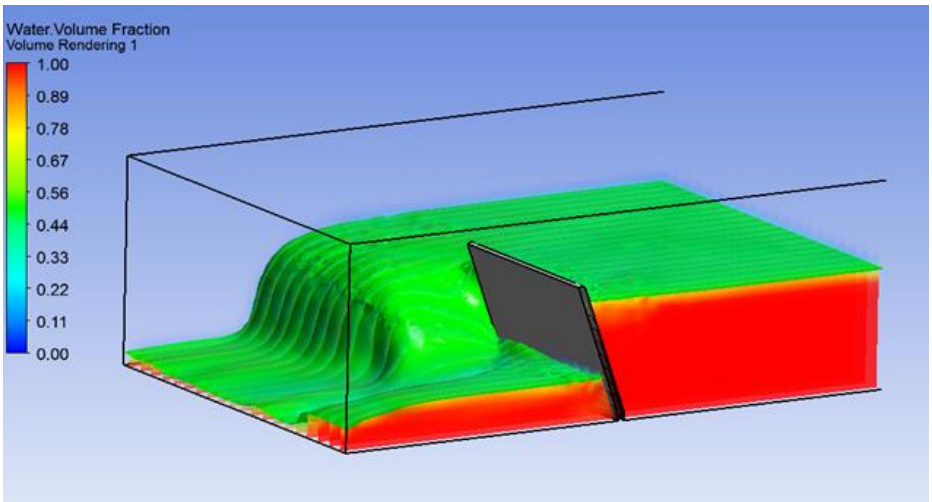

Fig. 9 Water surface profile over the weir with two gates

Table 4 Hydraulic parameters and weir discharge coefficient for two-gate pivot weirs

Geometry and hydraulics parameters		**Number of model runs**								
		1	**2**	**3**	**4**	**5**	**6**	**7**	**8**	**9**
Type		**L70- R50**			**L70 – R27.8**			**L50-R27.8**		
Discharge	Q (L/s)	130	80	40	130	80	40	130	80	40
Length of crest	b_L(cm)	60	60	60	60	60	60	60	60	60
	b_R(cm)	93.7	93.7	93.7	97.3	97.3	97.3	94.3	94.3	94.3
Angle ratio of right to left weirs	θ_r (degree)	0.71	0.71	0.71	0.40	0.40	0.40	0.56	0.56	0.56
Upstream Water depth	Y (cm)	44.2	41.1	37.6	38.9	32.3	25.7	36.9	32.5	27.0
Upstream Head over the crest	H_L(cm)	4.3	1.2	-2.3	-1.0	-7.6	-14.2	3.1	-1.3	-6.8
	H_R(cm)	10.4	7.3	3.8	16.2	9.6	3.0	14.2	9.8	4.3
Discharge coefficient	C_{L-1}	0.768	0.910	-	-	-	-	0.823	-	-
Discharge (Separately for each weir)	Q_L(L/s)	12	2	0	0	0	0	8	0	0
	Q_R(L/s)	118	78	40	130	80	40	122	80	40
Discharge coefficient	C_{R-1}	1.261	1.429	1.918	0.698	0.944	2.683	0.825	0.930	1.612
weighted average of discharge coefficient	C_{avg}	1.069	1.226	1.918	0.698	0.944	-	0.825	0.930	1.612
Left and right discharge coefficients with equal angles (Fig. 8)	C_{L-2}	0.768	0.910	-	-	-	-	0.823	-	-
	C_{R-2}	0.584	0.664	0.789	0.519	0.604	0.825	0.530	0.597	0.770
Flow rate increase ratio	N_L	1.0	1.0	-	-	-	-	1.0	-	-
	N_R	2.2	2.2	2.4	1.3	1.6	-	1.6	1.6	2.1

for the right-side crest (b_R) is defined to consider this increment. Therefore, an increase in b_R due to the weir angle reduction is related to flow rate growing, which is the sum of flow passes through the upper and side edge of the right weir. If the angle of two weirs is equal, the total length of the crest is 120 cm. By changing the right weir angle, the total weir length increases to 153.7 cm, 154.3 cm, and 157.3 cm (28.1%, 28.6%, and 31.1%), respectively.

In this study, the left weir angle is considered to be always greater (see Table 4). Therefore, the flow is only passes over its upper edge and hence the results of Fig. 8 was applied to calculate C_{L-1}, which was subsequently used in Eq. (1) to estimate Q_L. For low flows, where the water passes only through the right weir, C_{L-1} is zero. The flow over the right weir (Q_R) is also determined based on the difference between the total flow and Q_L. Afterward, the discharge coefficient for the right weir (C_{R-1}) is estimated using Q_R, H_R and b_R in Eq. (1). Figure 10 shows the results of head-discharge variation for the left and right weirs. The relation between discharge coefficients (C_{L-1}, C_{R-1} and C_{avg}) and H and H/P are also provided in Fig. 11 &12.

According to Fig. 10(a), the discharge-head variation of the left weir is in a good agreement with the experimental results, which illustrates the independency of Q_L-H_L relation from θ_r. Similar behavior for Q_L-H_L can be concluded in Fig. 10(b) with θ_r=1 (similar to single gate). For a certain value of H, if the angles of the weirs changes ($\theta_r \neq 1$), the flow discharge through the weirs increases significantly. Therefore, two curves of (Q_R-H_R) for the right weir are provided for θ_r=1 and $\theta_r \neq 1$. In Fig. 11 & 12, variations of C_{L-1}, C_{R-1} and C_{avg} with respect to H and H/P for left and right weirs are provided, which are in reasonable agreement with those of experiments. The figures express less consistency between C_{avg} and H and H/P parameters for both right and left weirs compared to C_{L-1} and C_{R-1} coefficients.

In Fig. 11(a) & 11(c), C_{L-1} and C_{avg} variations have less fluctuation and good convergence versus H_L. However, Fig. 11(b) & 11(d) show large variations and

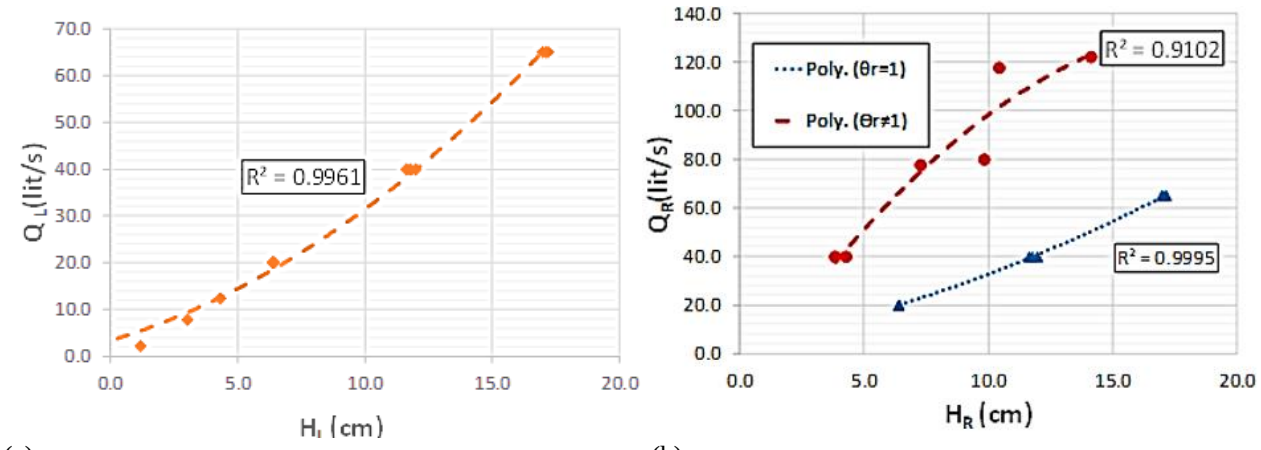

(a) (b)

Fig. 10 Variation of Q versus H

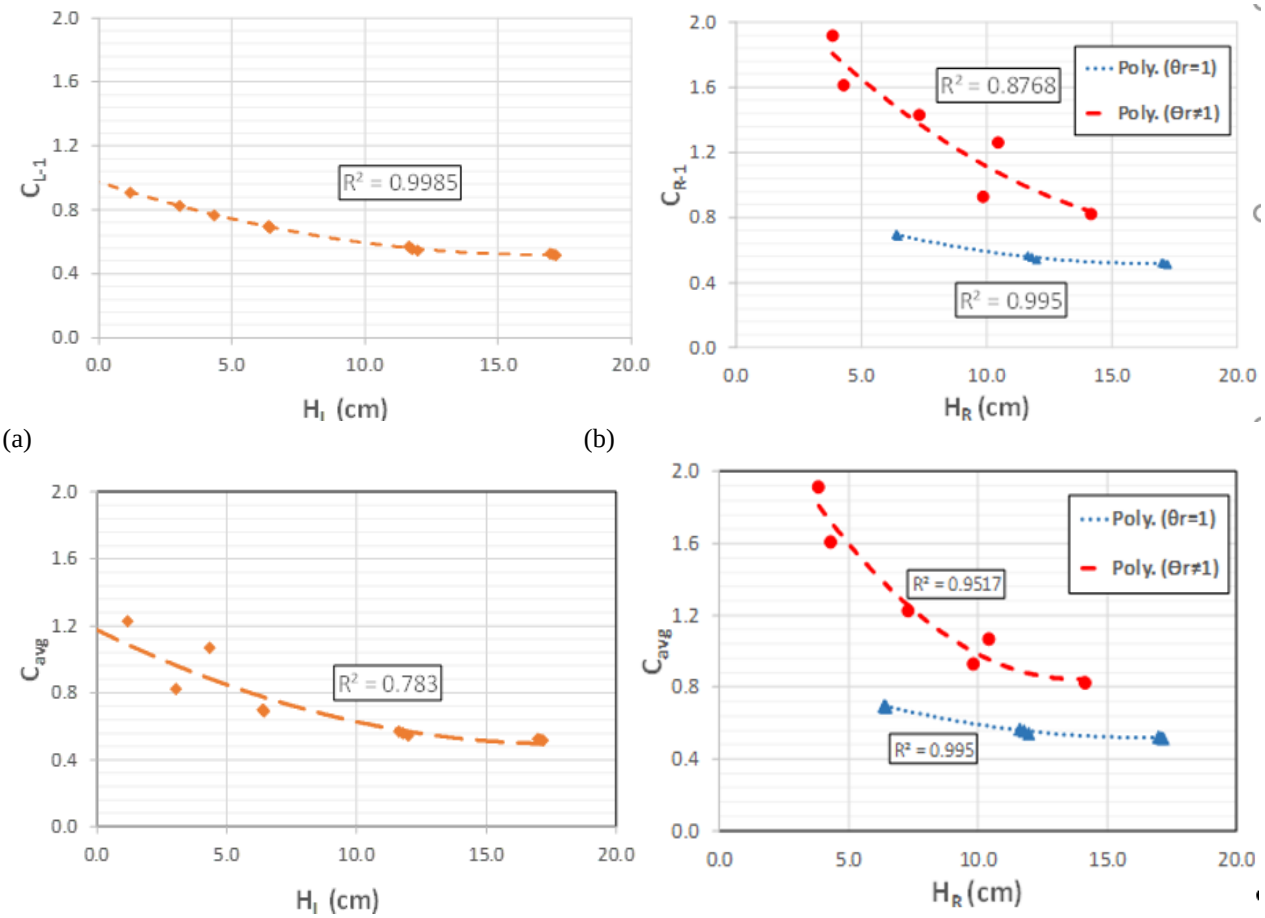

(a) (b)

(c) (d)

Fig. 11 Variation of C_{L-1}, C_{R-1} and C_{avg} versus H_L, H_R

fluctuations of these coefficients versus H_R. So, for the weir on the right side, two curves (C_{R-1}-H_R and C_{avg}-H_R) have been fitted separately for θ_r=1 and θ_r≠1. Also, in the conditions where θ_r=1, the discharge coefficient fluctuated slightly, but due to the difference in the angle between the two weirs (θ_r≠1), the value of C_R and subsequently C_{avg} increased significantly. For example, for H_R=10 cm, the C_R discharge coefficient for θ_r=1 and θ_r≠1 modes is 0.6 and 1.12, respectively. In other words, the weir discharge coefficient on the right depends on the angle of the weir on the left. Similarly, this issue can be seen in Fig. 12 in relation to H/P values.

Considering the importance of the angle ratio of the two weirs (θ_r) on the hydraulic characteristics, the variations of C_{avg} versus θ_r was determined for three different discharges and the results are provided in Fig. 13. As can be seen, C_{avg} increases first with increasing θ_r up to θ_r=0.7, but then reduces by further increasing of θ_r. Therefore, according to Table 4, in addition to θ_r, the values of θ_L and θ_R also show significant effect on C_{avg}.

In case, when the two adjacent weirs with different angles are considered in the waterway and the flow is not allowed to pass between the two weirs, the discharge

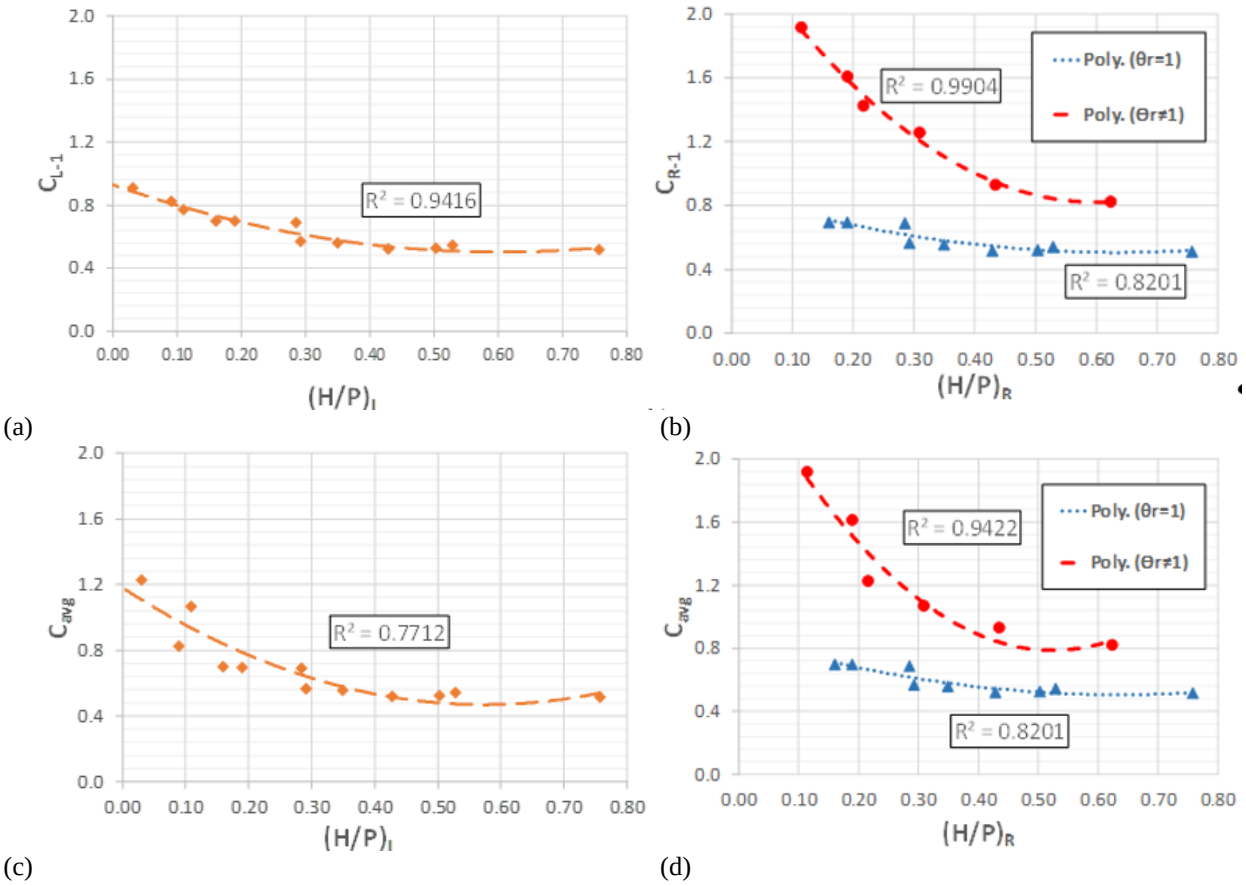

Fig. 12 Variation of C_L, C_R and C_{avg} versus H/p (L&R)

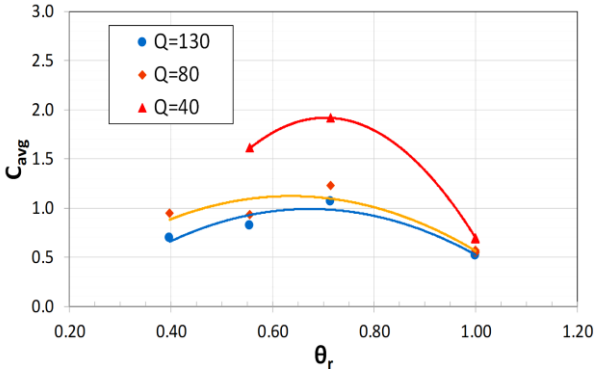

Fig. 13 Variation of C_{avg} versus θ_r

coefficients were calculated and compared with the present study.

3.3. Effect of a Retaining Wall (Third Step)

Without retaining wall, flow passes over the weirs and also through the open space between the two adjacent weirs (C_{L-1} and C_{R-1} values). However, if this open space is (virtually) blocked by a retaining wall, the flow reduces and is controlled by only the weirs (C_{L-2} and C_{R-2} is based on Fig. 8).

By determining the discharge coefficients for the two cases, the ratio of the discharge coefficients for the left (N_L) and right (N_R) weirs are determined.

The values of N_L and N_R (in Table 4) show that the discharge coefficient on the right side increases in the order of 1.3 and 2.4 times, due to the extra flow which [asses through the open space between the two gates or increase in the effective length of the weir.

Variation of water depth upstream of the weir with the flow discharge (Q-Y) for a series of weirs with a combination of angles (70°-50°) and (50°-27.8°) are shown in Fig. 14.

According to Fig. 14a, by 20° decrease in the right weir angle (L70-R70 to L70-R50), the upstream water depth decreases by 18.8% to 22.4%, depending upon the flow rate. The results of similar adjacent weir angles (L70-R70 to L50-50) show the upstream water depth reduction by 10.9% to 13.2%. The comparison of the two cases shows the importance of different operating angles for adjacent weirs on upstream water surface reduction during flood events. Similar behavior can be seen in Fig. 14b as well. By decreasing the weir angle on the right side (L50-R50 to L50-R27.8), the upstream water depth reduced by 22.8% to 28.7%. In the case of reduction angle (L50-R50 to L27.8-R27.8), the upstream depth reduces by 21.4% to 27.4%.

The upstream flow depth can also be related flow discharge (Q_R) passing over the right weir (Table 4). For example, by a 20° weir angle decrease in right weir (L70-R70 to L70-R50), the effective length of weirs increases by 28.1% and the flow discharge through the right weir increases (from 65 to 118 lit/s) by 81%. Therefore, pivot weirs show significant impact on reduction of their upstream flow depth and also on increasing flow discharge passing over, which illustrates an important effect on flow control and especially during flood events.

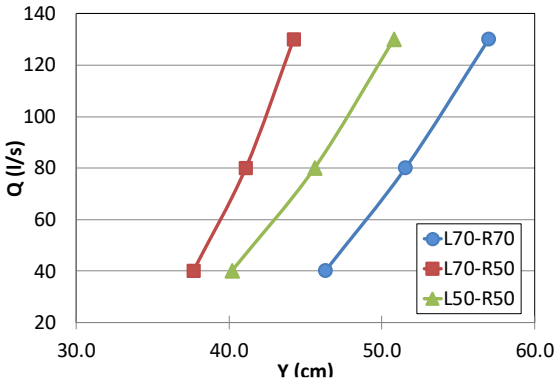

(a)

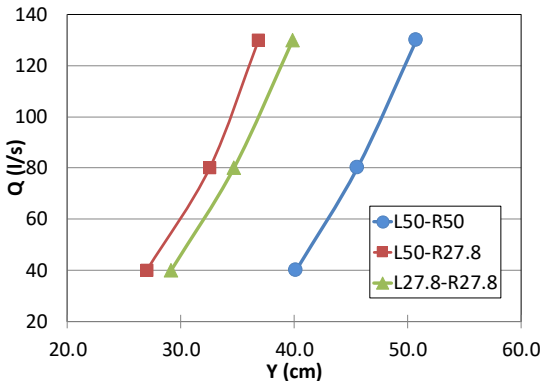

(b)

Fig. 14 The changes of flow discharge versus the water depth of the upstream flume

4. CONCLUSIONS

Given the point stated in above sections, due to the increasing development of pivot weirs and the need to utilize in different conditions (flood and drought events), examining the hydraulic performance of these types of weirs is a key prerequisite for the designers in different conditions. In this study, numerical simulation of two pivot weirs installed in a row in the channel bed was investigated. The structure of these weirs and lack of retaining wall between two adjacent weirs should be considered during their operation. When the angles of two weirs are equal, the whole structure acts as a single unit. Therefore, in the first step, the weirs with equal angles were analyzed, afterwards the results were incorporated in weirs with different angles. The following results emerged from this research:

For weirs with equal angles (θ_r=1), the experimental data showed a very good agreement with the results of Ansys CFX. The effective angle coefficient (C_a) first increases and then decreases by weir angle. The highest value of C_a equal to 1.076 was obtained for the weir angle of 52 degrees. In this case, the weir discharge coefficient increased by 7.6%. An equation for discharge coefficient were developed, considering the hydraulic parameters. The equations were used on which the angles of two weirs are different.

For weirs with unequal angles ($\theta_r \neq 1$), the results showed the increase of effective weirs length by 28.1% to 31.1%. As a result, the discharge coefficient for the weir with a lower angle increases by 1.3 to 2.4 times. By calculating the flow over two weirs and compare it with initial condition (θ_r=1) revealed that despite an increase in weir length, major flow is discharged over the right-side weir (with smaller angle). Analysis of Q-Y curves showed the efficiency of different adjacent weirs angles operation in the range of 5 to 10% than the operation of two weirs with similar angles. The results also showed that about 26% to 69% percent of the flow passing on the right weir passes through the distance between the two weirs. Therefore, in flood conditions, operation of pivot weirs with different angles is recommended for flood control.

References

Abdolahpour, M., Abbaspour A., Hasanpour, N., & Salmasi, F. (2013). *Numerical simulation of flow over rectangular broad-crested weir with upstream and downstream side slopes using fluent model*. 9th International River Engineering Conference, Shahid Chamran University.

Ahmed, S., & Aziz, W. (2018). Numerical modeling of flow in side channel spillway using ANSYS-CFX. *ZANCO Journal of Pure and Applied Sciences*, 30(s1), https://doi.org/10.21271/zjpas.30.s1.10

Arvanaghi, H., & Oskuei, N. (2013). Sharp-crested weir discharge coefficient. *Journal of Civil Engineering and Urbanism*, 3(3), 87-91.

Bijankhan, M., & Ferro, V. (2018). Experimental study and numerical simulation of inclined rectangular weirs. *Journal of Irrigation and Drainage Engineering*, 144(7), 04018012. https://doi.org/10.1061/(asce)ir.1943-4774.0001325

Godderidge, B., Phillips, A. B., Lewis, S., Turnock, S. R., Hudson, D. A., & Tan, M. (2004). *The simulation of free surface flows with Computational Fluid Dynamics*. ANSYS UK User Conference: Inspiring Engineering.

Gong, J., Deng, J., & Wei, W. (2019). Discharge coefficient of a round-crested weir. *Water* (Switzerland), 11(6). https://doi.org/10.3390/w11061206

Khatamipour, B., & Kavianpour, M.R, & Khosrojerdi, A., & Ghodsihassanabad, M. (2022a). Numerical Study of Flow Characteristics Over Pivot Weirs. Journal of Hydraulic Structures. https://doi.org/10.22055/jhs.2022.41058.1216

Khatamipour, B., & Khosrojerdi, A., & Kavianpour, M. R., & Ghodsihassanabad, M. (2022b). Simulation of two-phase turbulent flow of pivot weirs with different crest shapes. *Water and Soil Resources Conservation*. https://doi.org/10.30495/wsrcj.2022.19227

Kindsvater, C. E., & Carter, R. W. (1959). discharge characteristics of rectangular thin-plate weirs. *American Society of Civil Engineers (ASCE)* 124(1), 772-801.

Kulkarni, K. H., & Hinge, G. A. (2017, December 21- 23). *Compound broad crested weir for measurement of discharge – a novel approach, proceedings*, International Conference organized by Indian Society of Hydraulics – ISH HYDRO. India.

Kulkarni, K. H., & Hinge, G. A. (2020). Experimental study for measuring discharge through compound broad crested weir. *Flow Measurement and Instrumentation*. 75, 101803. https://doi.org/10.1016/j.flowmeasinst.2020.101803

Kulkarni, K. H., & Hinge, G. A. (2021). Performance enhancement in discharge measurement by compound broad crested weir with additive manufacturing, *Larhyss Journal*, 48, 169-188. http://larhyss.net/ojs/index.php/larhyss/index

Kulkarni, K. H., & Hinge, G. A. (2022). Comparative study of experimental and CFD analysis for predicting discharge coefficient of compound broad crested weir. *Water Supply*, 22(3), 3283-3296. https://doi.org/10.2166/ws.2021.403

Liu, C., Huhe, A., & Ma, W. (2002). Numerical and experimental investigation of flow over a semicircular weir. *Acta Mechanica Sinica/Lixue Xuebao*, 18(6), 594-602. https://doi.org/10.1007/bf02487961

Mahdavi, A., & Shahkarami, N. (2020). SPH Analysis of Free Surface Flow over Pivot Weirs. *KSCE Journal of Civil Engineering*, 24(4), 1183-1194. https://doi.org/10.1007/s12205-020-0095-1

Manz, D. H. (1985). *Systems analysis of irrigation conveyance systems*. [Master's thesis, University of Alberta]. Edmonton, AL, Canada.

Shawnm, M. S., & Sarhang, M. H. (2019). Validation of the computational ANSYS -CFX code for free surface flow: skimming flow over non-uniform step size stepped spillways. *Zanco Journal of Pure and Applied Sciences*, 31(s3), 361-367. https://doi.org/10.21271/zjpas.31.s3.51

Sheikh Rezazadeh, N., Monem, M. J., & Safavi, K. (2016). Extraction of the flow rate equation under free and submerged flow conditions in pivot weirs with different side contractions. *Journal of Irrigation and Drainage Engineering*, 142(8), 04016025. https://doi.org/10.1061/(asce)ir.1943-4774.0001027

Wahlin, B. T., & Replogle, J. A. (1994). *Flow measurement using an overshot gate*. U.S. Dept. of the Interior Bureau of Reclamation, Denver. https://doi.org/10.1080/09715010.2003.10514735

Zachoval, Z., & Roušar, L. (2015). *Flow structure in front of the broad-crested weir*. EPJ Web of Conferences (Vol. 92). EDP Sciences. https://doi.org/10.1051/epjconf/20159202117